



# Electrically pumped InP/GaAsP quantum dot lasers grown on (001) Si emitting at 750 nm

WEI LUO,<sup>1,2</sup>  LIYING LIN,<sup>1,2</sup>  JIE HUANG,<sup>1</sup>  QI LIN,<sup>1</sup> AND KEI MAY LAU<sup>1,\*</sup> 

<sup>1</sup>Department of Electronic and Computer Engineering, Hong Kong University of Science and Technology, Clear Water Bay, Kowloon, Hong Kong

<sup>2</sup>These authors contributed equally to this work

\*[eeekmlau@ust.hk](mailto:eeekmlau@ust.hk)

**Abstract:** Excellent performance of InAs quantum dot (QD) lasers grown on Si in the datacom and telecom bands has been reported in recent years. InP QD lasers on Si with emission wavelength at 650 nm–750 nm are seldom explored. In this paper, we report the growth and room temperature lasing of electrically pumped InP/GaAsP QD lasers directly grown on (001) Si emitting at 750 nm. The lowest threshold current density obtained is  $\sim 650$  A/cm<sup>2</sup>, measured on a 2 mm  $\times$  70  $\mu$ m device. Moreover, the highest operating temperature of the InP QD laser grown on the GaAs/Si template is above 95°C. This 750 nm near red on-chip light source for the monolithic integration of Si photonics is potentially applicable in display, bio-photonics, and spatial mapping.

© 2022 Optica Publishing Group under the terms of the [Optica Open Access Publishing Agreement](#)

## 1. Introduction

Si photonics has witnessed unprecedented advancement in telecom communication due to the large bandwidth and potential compatibility with the CMOS process [1]. Remarkable progress has been made on devices fabricated on Si for the monolithic integration, including waveguide [2], photodetector [3], and the most challenging device: laser [4,5]. Presumably less sensitive to defects generated in hetero-epitaxial growth, QDs have been used in the active region of III-V lasers grown on Si with impressive device performance [6]. The development of a visible light source grown on Si lags behind, despite the need has been demonstrated in visible photonics integrated circuits heterogeneously on Si with low loss SiN<sub>x</sub> waveguide [7]. Although red-emitting InP/AlGaInP QD lasers grown by metal-organic chemical vapor deposition (MOCVD) have achieved progressive performance, they are all demonstrated on the native GaAs substrate [8,9]. Recently, Dhingra et al. have demonstrated an electrically pumped InP/AlGaInP QD laser on Si emitting at  $\sim 726$  nm by molecular beam epitaxy (MBE) [10]. However, typical (Al)GaInP materials suffer from ordering in epitaxial growth, which changes their bandgap and causes a rough surface [11,12]. The degree of ordering can be reduced by growing the (Al)GaInP on GaAs with an offcut angle [13], which was widely used in AlGaInP-based red laser and light emitting diode (LED) [14–16]. However, substrates with an offcut angle are incompatible with the CMOS process and silicon photonics with passive devices demonstrated on (001) Si.

High-performance GaAsP/AlGaAs QW lasers were demonstrated on GaAs with a broad tunable emission wavelength between 715 nm and 790 nm [17,18]. To take advantage of the known benefits of growing QD lasers on silicon, we have explored the potential of embedding InP QDs in the simple ternary GaAsP/AlGaAs QW system on (001) Si by MOCVD. Combined with the low defect density GaAs/Si templates we developed in-house, room temperature pulse lasing of the InP/GaAsP dot-in-well (DWELL) structure laser has been achieved. The lowest threshold current density of the InP QD laser grown on GaAs and GaAs/Si template is 573 A/cm<sup>2</sup> and 657 A/cm<sup>2</sup>, respectively, obtained on two 2 mm  $\times$  70  $\mu$ m devices. Furthermore, the highest

operating temperatures of the laser on GaAs and GaAs/Si templates are all above 95°C, which is limited by the setup.

## 2. Experiment

The electrically pumped InP/GaAsP QD laser was grown on CMOS-compatible nominal (001) Si by MOCVD. The laser structure was grown in a horizontal reactor MOCVD (AIXTRON 200/4), while the GaAs/Si templates were grown in another one (AIXTRON CCS). Prior to the growth of the GaAs on Si, high temperature (800°C) annealing was performed in H<sub>2</sub> ambient to form the double atomic steps and remove the native oxide [19]. To reduce the defects introduced by the lattice mismatch between GaAs and Si, six cycles of thermal cycle annealing (TCA) were performed with temperatures cycling between 730°C and 330°C after the growth of 1 μm GaAs. In addition, ten periods of 9.3 nm In<sub>0.15</sub>GaAs/12 nm GaAs strain layer superlattices (SLSs) were inserted in the GaAs to bend the propagation of threading dislocations (TD). The total thickness of the GaAs/Si template is 2 μm, which is a tradeoff between the TD density and the generation of cracks. The TD density of the GaAs/Si template is  $2.8 \times 10^7/\text{cm}^2$ , and its surface roughness is 1.3 nm, measured by an atomic force microscope (AFM).

Using the GaAs/Si templates, 700 nm n-doped GaAs was grown as a contact layer, followed by 800 nm Al<sub>0.7</sub>Ga<sub>0.3</sub>As cladding. Then a five-layer stack of InP QDs were grown in the GaAs<sub>0.6</sub>P<sub>0.4</sub> QW and spaced by 20 nm Al<sub>0.4</sub>Ga<sub>0.6</sub>As, which were sandwiched by 80 nm Al<sub>0.4</sub>Ga<sub>0.6</sub>As barrier. Finally, an 800 nm Al<sub>0.7</sub>Ga<sub>0.3</sub>As cladding and 300 nm p-doped GaAs were grown on top of the structure. The doping concentration of n-GaAs contact, n-Al<sub>0.7</sub>Ga<sub>0.3</sub>As cladding, p-Al<sub>0.7</sub>Ga<sub>0.3</sub>As cladding, and p-GaAs contact is  $1 \times 10^{19}/\text{cm}^3$ ,  $6.9 \times 10^{17}/\text{cm}^3$ ,  $1.6 \times 10^{18}/\text{cm}^3$ , and  $4.6 \times 10^{19}/\text{cm}^3$ , respectively. Optimization of the QD laser growth was performed on GaAs substrates.

The schematic of the InP/GaAsP QD grown on GaAs substrate is shown in Fig. 1(a), which consists of multi-layer QDs. The InP QDs are grown at 680°C on the tensile strained 4 nm GaAsP QW, and the V/III ratio of the QD is 16. Then the QDs are capped by another 4 nm GaAsP QW grown at 650°C to form the DWELL structure. Each layer of InP/GaAsP QD was separated by a 20 nm Al<sub>0.4</sub>Ga<sub>0.6</sub>As barrier. After the growth of the final 60 nm Al<sub>0.4</sub>Ga<sub>0.6</sub>As barrier, another layer of InP/GaAsP QD was grown on top for morphology characterization of the QDs. The QD samples are measured by the μPL setup with a 514 nm continuous-wave (CW) diode laser and a charged-coupled device (CCD) detector. The pumping power is 25 mW and the spot diameter of the laser is ~2 μm, which can characterize the performance of the localized QDs. As shown in Fig. 1(b), the μPL intensity of the InP/GaAsP QD grown at 680°C is almost four times of that grown at 690°C. From the AFM image of the top exposed InP QDs shown in Figs. 2(a) and 2(b), the morphology of the QD changes drastically with different growth temperatures due to the changed critical thickness for the formation of QDs. But the InP/GaAsP QD grown at 680°C and 690°C show a similar QD density of  $\sim 1.6 \times 10^{10}/\text{cm}^2$ . In addition, the μPL intensity of the InP/GaAsP QD is further improved by increasing the stacking layers from 3-layer to 5-layer as shown in Fig. 1(c).

The center wavelength of the 5-layer InP/GaAsP QD is ~736 nm. The AFM image of the 5-layer InP/GaAsP QD is shown in Fig. 2(c) with a QD density of  $\sim 7.0 \times 10^9/\text{cm}^2$ . The changed morphology and somewhat reduced QD density compared with the 3-layer InP/GaAsP QD were caused by the accumulated strain through increasing the number of stacked tensile strained GaAsP QW layers.

Based on the optimized InP/GaAsP QD, the complete laser structure (Fig. 3(a)) was grown on the GaAs/Si templates, simultaneously with GaAs substrates distributed on the susceptor. The AFM images of the electrically pumped InP/GaAsP QD laser grown on GaAs and GaAs/Si templates are shown in Figs. 3(b) and 3(c), with a surface roughness of 0.18 nm and 2.76 nm, respectively. A cross-sectional transmission electron microscope (TEM) image of the electrically

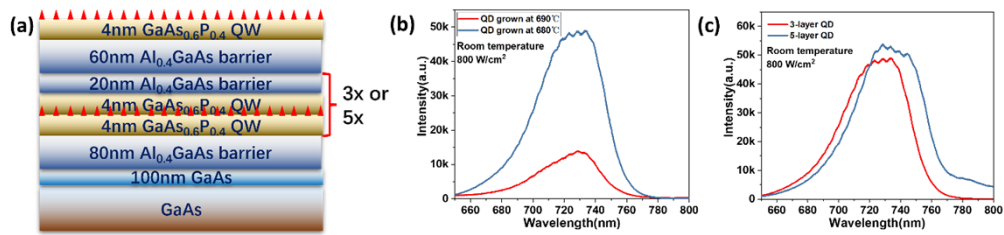


**Fig. 1.** (a) Schematic of the InP/GaAsP QD grown on GaAs substrate; (b)  $\mu$ PL of the InP/GaAsP QD grown at 690°C and 680°C on GaAs substrate. (c)  $\mu$ PL of the 3-layer and 5-layer InP/GaAsP QD grown on GaAs substrate. The  $\mu$ PL was measured at room temperature.

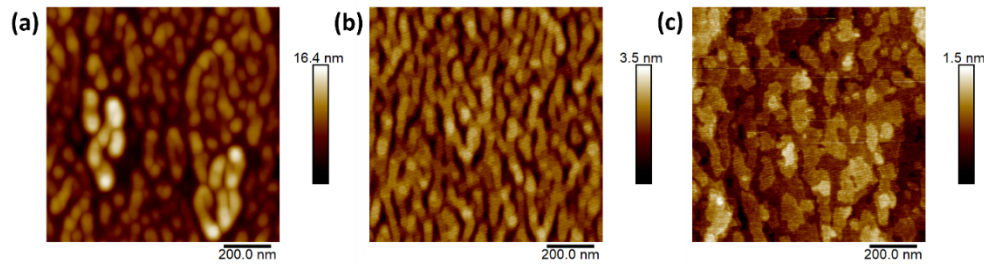


**Fig. 2.** AFM images of the 3-layer InP/GaAsP QD grown at (a) 690°C and (b) 680°C on GaAs substrate. (c) AFM image of the 5-layer InP/GaAsP QD grown at 680°C on GaAs substrate.

pumped InP/GaAsP QD laser grown on the GaAs/Si template is shown in Fig. 3(d), with a zoomed-in image of the InP QDs shown in Fig. 3(e).

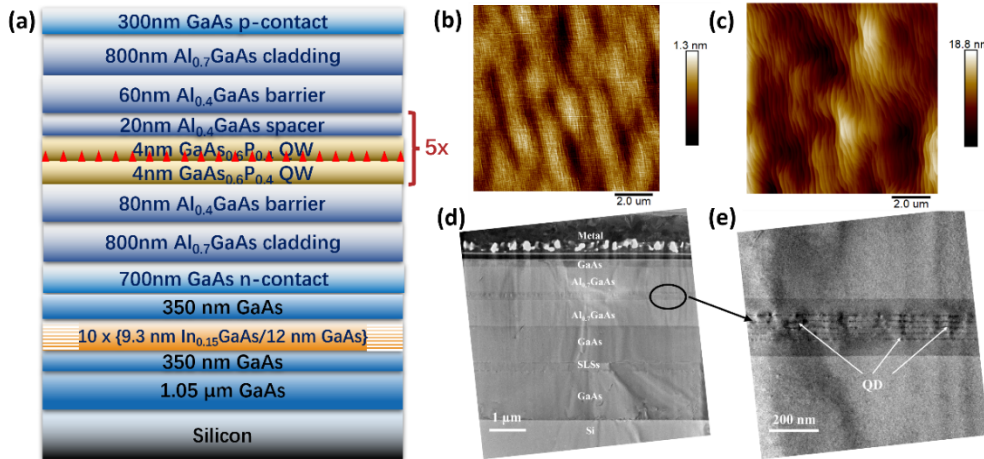


**Fig. 3.** (a) Schematic of the electrically pumped InP/GaAsP QD laser grown on the GaAs/Si template. AFM images of the electrically pumped InP/GaAsP QD laser grown on (b) GaAs and (c) GaAs/Si templates with the surface roughness of 0.18 nm and 2.76 nm, respectively. (d) Cross-sectional TEM images of the electrically pumped InP/GaAsP QD laser grown on the GaAs/Si template. (e) Zoom-in cross-sectional TEM image of the InP/GaAsP QD.

### 3. Result and discussion

The as-grown samples were fabricated into ridge waveguide edge-emitting lasers to investigate the device performance of the InP/GaAsP QD laser. The detailed fabrication process of the laser was described in [20]. The fabricated laser bars were placed on a heated stage with a temperature controller for temperature-dependent measurement. A pulsed current source with a duty cycle of 0.5% and a pulse width of 400 ns was used for the device measurement. As shown in Fig. 4(a), the current-voltage (I-V) characteristics of representative InP QD lasers grown on GaAs and GaAs/Si templates are very similar, with a turn-on voltage of 1.4 V and a resistance of 8.8-11.7  $\Omega$ . To compare the optical performance of lasers on GaAs and GaAs/Si templates, light-current (L-I) curves of InP/GaAsP QD laser measured at 20°C with different dimensions are shown in Fig. 4(b). The threshold current density of the same size InP/GaAsP QD lasers grown on GaAs and GaAs/Si templates are comparable, which reflects the high material quality of QD laser grown on Si. The threshold current density of larger size devices is smaller due to the higher net gain to overcome the optical losses [21]. The lowest threshold current density of the InP/GaAsP QD lasers grown on GaAs and GaAs/Si templates is 573 A/cm<sup>2</sup> and 657 A/cm<sup>2</sup>, respectively, obtained on the 2 mm  $\times$  70  $\mu$ m devices.

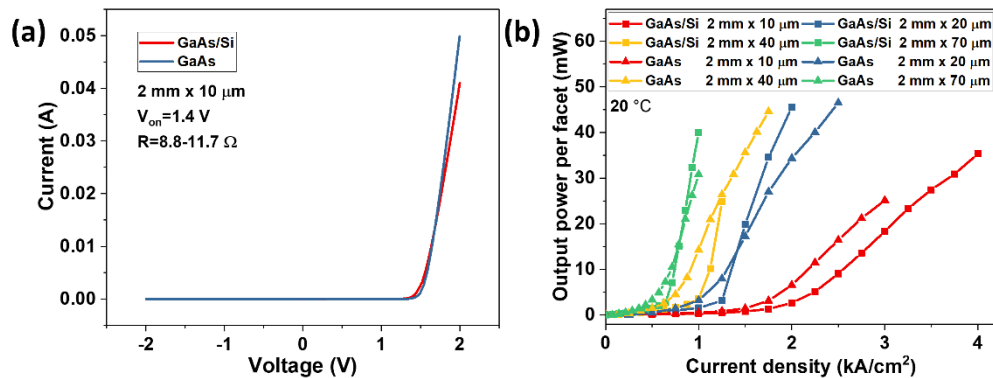


**Fig. 4.** (a) Representative I-V curves of the InP/GaAsP QD laser grown on GaAs and GaAs/Si templates. (b) L-I curves of the InP/GaAsP QD laser grown on GaAs and GaAs/Si templates with different dimensions.

Temperature-dependent L-I curves of 2 mm  $\times$  10  $\mu$ m InP/GaAsP QD lasers grown on GaAs and GaAs/Si templates are shown in Figs. 5(a) and 5(b), respectively. The QD laser grown on both substrates can lase above 95°C, which is the limitation of the measurement setup. As shown in Fig. 5(c), the characteristic temperature of the InP/GaAsP QD laser grown on GaAs and GaAs/Si templates is 62 K and 74 K, respectively. The characteristic temperature of the InP/GaAsP QD laser grown on the GaAs/Si template is higher than that on GaAs, which may be a result of better thermal dissipation of Si. The emission spectra at progressively increased currents of the 2 mm  $\times$  10  $\mu$ m InP/GaAsP QD laser grown on the GaAs/Si template are shown in Fig. 6. The spectra were measured at 20°C with a peak wavelength of  $\sim$ 757 nm.

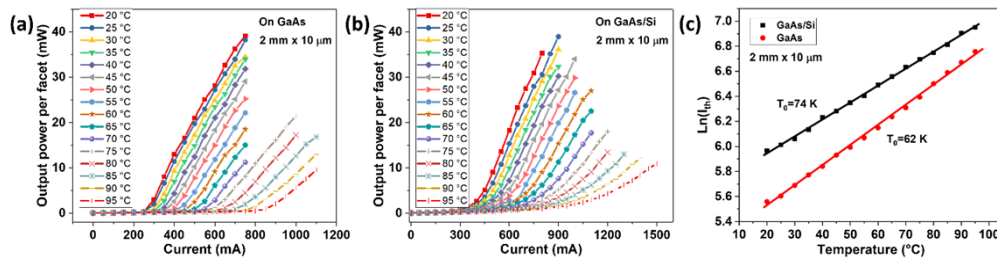


**Fig. 5.** (a) Temperature-dependent L-I curves of the  $2 \text{ mm} \times 10 \text{ }\mu\text{m}$  InP/GaAsP QD lasers grown on (a) GaAs and (b) GaAs/Si templates, respectively. (c) Characteristic temperature of the  $2 \text{ mm} \times 10 \text{ }\mu\text{m}$  InP/GaAsP QD lasers grown on GaAs and GaAs/Si templates.

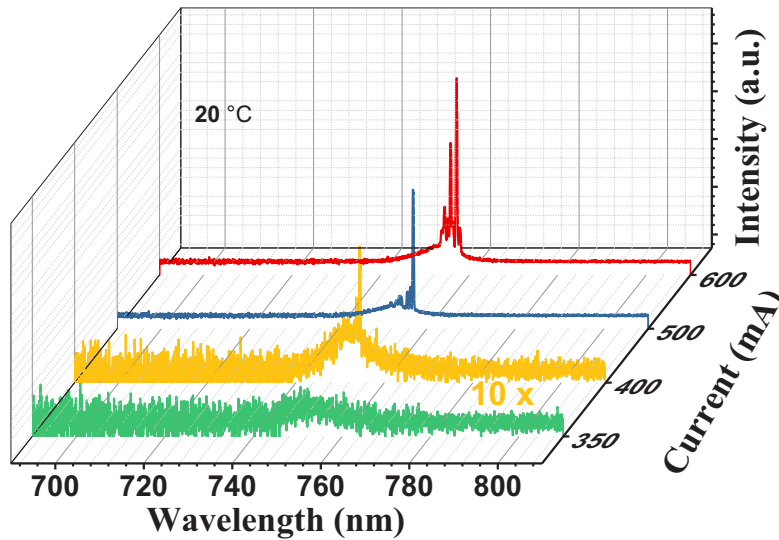


**Fig. 6.** Emission spectra at progressively increased currents of the  $2 \text{ mm} \times 10 \text{ }\mu\text{m}$  InP/GaAsP QD laser grown on the GaAs/Si template measured at  $20 \text{ }^\circ\text{C}$ .

#### 4. Conclusion

In conclusion, we demonstrated electrically pumped InP/GaAsP QD lasers grown on (001) Si with pulsed lasing at room temperature. Initial results here show comparable device performance on GaAs and GaAs/Si templates with the lowest threshold current density of  $573 \text{ A/cm}^2$  and  $657 \text{ A/cm}^2$ , respectively. The highest operating temperature of the InP/GaAsP QD laser is above  $95 \text{ }^\circ\text{C}$  on GaAs and GaAs/Si templates with characteristic temperatures of 62 K and 74 K. Embedding InP QDs in the simple ternary GaAsP/AlGaAs QW systems provides an efficient and reliable light source with emission wavelength at  $\sim 750 \text{ nm}$  on Si, paving the way toward the integration with Si photonics for a variety of applications near the infrared.

**Funding.** Innovation and Technology Fund (ITS/201/19FP).

**Acknowledgments.** The authors would like to thank Nanosystem Fabrication Facility (NFF) and the Material Characterization & Preparation Facility (MCPF) of HKUST for their technical support.

**Disclosures.** The authors declare no conflicts of interest.

**Data availability.** Data underlying the results presented in this paper are not publicly available at this time but may be obtained from the authors upon reasonable request.

## References

1. N. Margalit, C. Xiang, S. M. Bowers, A. Bjorlin, R. Blum, and J. E. Bowers, "Perspective on the Future of Silicon Photonics and Electronics," *Appl. Phys. Lett.* **118**(22), 220501 (2021).
2. N. L. Kazanskiy, M. A. Butt, and S. N. Khonina, "Silicon Photonic Devices Realized on Refractive Index Engineered Subwavelength Grating Waveguides-A Review," *Opt. Laser Technol.* **138**, 106863 (2021).
3. Y. Xue, Y. Wang, W. Luo, J. Huang, L. Lin, H. K. Tsang, and K. M. Lau, "Telecom InP-Based Quantum Dash Photodetectors Grown on Si," *Appl. Phys. Lett.* **118**(14), 141101 (2021).
4. Y. Wan, C. Xiang, J. Guo, R. Kosciwa, M. Kennedy, J. Selvidge, Z. Zhang, L. Chang, W. Xie, D. Huang, A. C. Gossard, and J. E. Bowers, "High Speed Evanescent Quantum Dot Lasers on Si," *Laser Photonics Rev.* **15**(8), 2100057 (2021).
5. C. Shang, E. Hughes, Y. Wan, M. Dumont, R. Kosciwa, J. Selvidge, R. Herrick, A. C. Gossard, K. Mukherjee, and J. E. Bowers, "High-Temperature Reliable Quantum-Dot Lasers on Si with Misfit and Threading Dislocation Filters," *Optica* **8**(5), 749 (2021).
6. V. Cao, J.-S. Park, M. Tang, T. Zhou, A. Seeds, S. Chen, and H. Liu, "Recent Progress of Quantum Dot Lasers Monolithically Integrated on Si Platform," *Front. Phys.* **10**, 839953 (2022).
7. M. A. G. Porcel, A. Hinojosa, H. Jans, A. Stassen, J. Goyvaerts, D. Geuzebroek, M. Geiselman, C. Dominguez, and I. Artundo, "[INVITED] Silicon Nitride Photonic Integration for Visible Light Applications," *Opt. Laser Technol.* **112**, 299–306 (2019).
8. Z. Li, C. P. Allford, S. Shutts, A. F. Forrest, R. Alharbi, A. B. Krysa, M. A. Cataluna, and P. M. Smowton, "Monolithic InP Quantum Dot Mode-Locked Lasers Emitting at 730 nm," *IEEE Photonics Technol. Lett.* **32**(17), 1073–1076 (2020).
9. Z. Huang, M. Zimmer, S. Hepp, M. Jetter, and P. Michler, "Optical Gain and Lasing Properties of InP/AlGaInP Quantum-Dot Laser Diode Emitting at 660 nm," *IEEE J. Quantum Electron.* **55**(2), 1–7 (2019).
10. P. Dhingra, P. Su, B. D. Li, R. D. Hool, A. J. Muhowski, M. Kim, D. Wasserman, J. Dallesasse, and M. L. Lee, "Low-Threshold InP Quantum Dot and InGaP Quantum Well Visible Lasers on Silicon (001)," *Optica* **8**(11), 1495 (2021).
11. T. Suzuki, A. Gomyo, S. Iijima, K. Kobayashi, S. Kawata, I. Hino, and T. Yuasa, "Band-Gap Energy Anomaly and Sublattice Ordering in GaInP and AlGaInP Grown by Metalorganic Vapor Phase Epitaxy," *Jpn. J. Appl. Phys.* **27**(Part 1, No. 11), 2098–2106 (1988).
12. K. L. Schulte, D. R. Diercks, D. M. Roberts, P. C. Dippe, C. E. Packard, J. Simon, and A. J. Ptak, "Effect of Hydride Vapor Phase Epitaxy Growth Conditions on the Degree of Atomic Ordering in GaInP," *J. Appl. Phys.* **128**(2), 025704 (2020).
13. L. C. Su, I. H. Ho, and G. B. Stringfellow, "Effects of Substrate Misorientation and Growth Rate on Ordering in GaInP," *J. Appl. Phys.* **75**(10), 5135–5141 (1994).
14. H. Hamada, "Characterization of Gallium Indium Phosphide and Progress of Aluminum Gallium Indium Phosphide System Quantum-Well Laser Diode," *Materials* **10**(8), 875 (2017).
15. J.-R. Dong, J.-H. Teng, S.-J. Chua, B.-C. Foo, Y.-J. Wang, H.-R. Yuan, and S. Yuan, "650-nm AlGaInP Multiple-Quantum-Well Lasers Grown by Metalorganic Chemical Vapor Deposition Using Tertiarybutylphosphine," *Appl. Phys. Lett.* **83**(4), 596–598 (2003).
16. G. Wang, X. Yi, T. Zhan, and Y. Huang, *The AlGaInP/AlGaAs Material System and Red/Yellow LED, in Light-Emitting Diodes*, J. Li and G. Q. Zhang, eds. Vol. 4 (Springer International Publishing, Cham, 2019), pp. 171–202.
17. G. Erbert, F. Bugge, A. Knauer, J. Sebastian, A. Thies, H. Wenzel, M. Weyers, and G. Trankle, "High-Power Tensile-Strained GaAsP-AlGaAs Quantum-Well Lasers Emitting between 715 and 790 nm," *IEEE J. Select. Topics Quantum Electron.* **5**(3), 780–784 (1999).
18. F. Agahi, A. Baliga, K. M. Lau, and N. G. Anderson, "Dependence of Polarization Mode and Threshold Current on Tensile Strain in AlGaAsGaAsP Quantum Well Lasers," *Solid-State Electron.* **41**(4), 647–649 (1997).
19. Q. Li, H. Jiang, and K. M. Lau, "Coalescence of Planar GaAs Nanowires into Strain-Free Three-Dimensional Crystals on Exact (001) Silicon," *J. Cryst. Growth* **454**, 19–24 (2016).
20. Y. Xue, W. Luo, S. Zhu, L. Lin, B. Shi, and K. M. Lau, "1.55  $\mu\text{m}$  Electrically Pumped Continuous Wave Lasing of Quantum Dash Lasers Grown on Silicon," *Opt. Express* **28**(12), 18172 (2020).
21. L. V. Asryan and R. A. Suris, "Inhomogeneous Line Broadening and the Threshold Current Density of a Semiconductor Quantum Dot Laser," *Semicond. Sci. Technol.* **11**(4), 554–567 (1996).